Peer-reviewed version available at Pharmaceutics 2018, 10, 259; doi:10.3390/pharmaceutics10040259

Article

Investigation of disintegration and dissolution behavior of mefenamic acid drug formulation using numeric solution of Noyes-Whitney equation with cellular automata model on microtomographic surfaces and rational arrangements of tablet components.

Reiji Yokoyama[1,2], Go Kimura[2], Christian Schlepütz[3], Jörg Huwyler[1], Maxim Puchkov[1]*

[1] Department of Pharmaceutical Sciences, Division of Pharmaceutical Technology, University of Basel, Klingelbergstrasse 50, CH4056 Basel, Switzerland
[2] Formulation R&D Center, CMC R&D Division, SHIONOGI & CO., LTD., Hyogo, Japan, E-mail: reiji.yokoyama@shionogi.co.jp
[3] Paul Scherer Institute, Villingen, Switzerland, E-mail: christian.schlepuetz@psi.ch
* Correspondence: E-mail: maxim.puchkov@unibas.ch; Tel.: +41 61 207 1619

Abstract: There are numerous approaches to model an influence of manufacturing parameters on the dissolution and disintegration of solid dosage forms. A modern approach for modelling and simulating complex and heterogeneous systems such as pharmaceutical tablets focuses on computationally-intensive finite-element or discreet element methods. Industrial challenges such as Process Analytical Technology (PAT) and Quality by Design are stimulating computer-based technologies to design, control and improve the quality of pharmaceutical compacts and their performance. In this study the disintegration and dissolution model based on the numerical solutions of the Noyes-Whitney equation and cellular automata supported disintegration model are proposed and evaluated. The results from *in vitro* release studies of the mefenamic acid formulations were compared to the calculated release patterns from the tablet structures obtained from microtomography experiments and the purely algorithmically created virtual tablets.

Keywords: drug release simulation, disintegration simulation, poorly water soluble drug, mefenamic acid, Noyes-Whitney equation, cellular automata, synchrotron microtomography

1. Introduction

Many different types of simulation have been developed to model the mechanical and dissolution behaviour of particles and tablets [1,2] and to also understand the key factors that affect the drug product quality. For example, Finite Element Method (FEM), in which the powder is treated as a continuous material, has been used to simulate the mechanical behaviour such as stress distribution and density distribution of tablets during compaction [3] and to simulate the drug release from hydrogel-based matrix tablets [4]. The Discrete Element Method (DEM) has been applied to simulate the swelling and dissolution of the hydrophilic polymer tablet with different tablet shape, component and drug loading [5–8] and has also been applied to characterize the breakage of agglomerates and tablets [9,10]. In addition, DEM and FEM hybrid models have been developed for particle breakage and compaction simulation [11,12]. Ideally, DEM requires a large number of virtual particles to take into account the microstructure and component heterogeneity of pharmaceutical tablets [5,13]. However, it is computationally expensive, due to a requirement to calculate physical and chemical interaction for all individual particles in the system [14]. Therefore, DEM is often using

Peer-reviewed version available at Pharmaceutics 2018, 10, 259; doi:10.3390/pharmaceutics10040259

larger spatial subdivisions, i.e., smaller number of larger particles as compared to those in reality [15]. In addition, a knowledge about numerous input parameters is necessary to simulate complex systems with DEM. The DEM model needs to be validated experimentally, which can be difficult [14]. The cellular automata algorithm has been proposed as a modelling technique [16,17], and it has been applied to simulate the drug release of tablets [18,19]. Three-dimensional cellular algorithms allow the calculation of matrices containing several components organized a large number of discrete cubes; this is possible due to the simplicity of the calculation, as compared to DEM models [14]. For example, it has been reported that the disintegration time of tablets [20], buoyancy and drug release profiles of gastroretentive floating tablets [21,22] were simulated with the three-dimensional cellular automata algorithm.

Drug release of tablets is influenced by the solubility of the active pharmaceutical ingredient (API) [23,24], particle size distribution [25], granule size and their arrangement [26–28]. In addition, it is well known that the drug release of the pharmaceutical tablets can be influenced by the tablet porosity due to change in disintegration behaviour of tablet, i.e. tablet disintegration time increase with a decrease in tablet porosity, resulting in a slow water penetration into tablet [29,30]. Furthermore, in general, the tablet porosity can be variable due to the batch-to-batch difference in compressibility of the powders/granules and variation of compressive stress in the high-speed tablet compaction. Therefore, from the formulation and process development and quality assurance point of view, the development of tools for computational elucidation of material attributes and production process influence on drug release is very important.

Validation of the simulation results is a challenging topic, mostly arising from an inability to describe the internal structure of a tablet in sufficiently precise way, i.e., including internal structures at simulation resolution. This challenge is addressed with X-ray computed microtomography, which is a technology to visualize the three-dimensional structure of compacts, and it has been applied to visualize the internal pore structure of the tablet and quantitate the density distribution [31,32]. And it has also been applied to elucidate the correlation between tablet internal structure and dissolution behaviour [33–35].

The purpose of this study is to simulate the dissolution and disintegration behaviour of a poorly soluble drug formulation applying numeric solutions for dissolution calculation based on Noyes-Whitney equation and cellular automata model for tablet disintegration. The influence of components' particle arrangement and tablet porosity on drug release profiles has been investigated by simulation of drug release from microtomographic three-dimensional surfaces of real tablets and from arrangements obtained with three-dimensional cellular automata algorithm. A combined approach for modelling complex multilevel physical process such as dissolution-disintegration has been proposed.

2. Materials and Methods

2.1 Materials

Mefenamic acid (SIGMA, USA) was used as a model compound to prepare rapid disintegrating tablets. The excipients used were D-mannitol (Pearlitol 25C, Roquette, France) and microcrystalline cellulose (Avicel PH-101, FMC bioPolymer, USA) as diluents, croscarmellose sodium (Ac-Di-Sol, FMC bioPolymer, USA) as disintegrant, Hydroxypropyl cellulose (HPC SL, NIPPON SODA, Japan) as binder and magnesium stearate (Peter Greven GmbH & Co, Germany) as a lubricant. Cetyltrimethylammonium bromide (CTAB) (Merck, USA) was used as a surfactant for disintegration tests and dissolution tests.

2.2 Methods

2.2.1 Preparation of tablets

The formulation of mefenamic acid tablet of 250 mg used for this study was prepared according to Table 1. Mefenamic acid, D-mannitol, microcrystalline cellulose and croscarmellose sodium were

weighted and granulated in a high-shear mixer (MYCROMIX, OYSTAR Hüttlin, Germany). The powders were pre-mixed for 1 min at an impeller speed of 250 rpm. Next, the granulation process was carried out at 250 rpm of impeller speed with chopper speed of 2000 rpm. Hydroxypropyl cellulose solution (10% w/w) was added at a spray rate of approx. 5 g/min. After adding the binding solution, water was added at the same spray rate to flush the line. The process was continued for 1 min. The obtained wet-granulates were dried and milled using screen mill (Fitz mill model L1A, Fitz Patrick, USA). Afterwards, the milled granules were mixed with croscarmellose sodium and magnesium stearate as an external phase. Tablets were compressed using a compaction simulator (StylOne, Medel pharma, France). The target dwell-time for pre-compression and main-compression were set to 25 ms. The compaction parameters are shown in Table 1. An 11.28 mm round flat-faced punch set was used for the preparation of formulation.

2.2.2 Determination of tablet porosity and tensile strength

Mean tablet weight was evaluated with an electronic balance (AX204 Delta Range, Mettler Toledo, Switzerland). In addition, tablet diameter and tablet thickness were evaluated with a digital caliper (CD-15CPX, Mitutoyo, Japan). All obtained values of tablet weight, diameter and thickness were within 1% deviation. True densities of all raw materials were evaluated using helium pycnometry (AccuPyc 1330, Micrometrics, USA). The values are given in Table 1.

Table 1. Formulation compositions and tablet compaction parameters (A1-A4)

		Formulation			
Formulation Composition	True density (g/cm^3)	mg		%, w/w	
Granular Composition					
Mefenamic acid	1.2554	250.0		50.0	
D-mannitol	1.4888	165.0		33.0	
Microcrystalline cellulose	1.5701	50.0		10.0	
Croscarmellose sodium	1.5757	10.0		2.0	
Hydroxypropyl cellulose	1.2334	15.0		3.0	
Granulate	-	490.0		98.0	
External Phase Composition					
Croscarmellose sodium	1.5757	5.0		1.0	
Magnesium stearate	1.0539	5.0		1.0	
Tablet weight	-	500.0		-	
Tablet Parameters (N=9)	-	A1*	A2	A3	A4
Tablet porosity (%, v/v)	-	6	9	14	23
Compressive stress (MPa)	-	210	150	99	45

* Indicates tablet formulation from composition A compressed at 210MPa

True density of tablets were calculated according to Eq. (1).

$$\rho_{tablet} = \frac{1}{\sum_{i=1}^{n} \frac{X_i}{\rho_i}} \quad (1)$$

Peer-reviewed version available at Pharmaceutics 2018, 10, 259; doi:10.3390/pharmaceutics10040259

where ρ_{tablet} and ρ_i are the true densities (g/cm^3) of the tablet and each raw material in the tablet, respectively, X_i are the weight fractions of each component.

Porosity ε of the tablets were determined according to Eq. (2).

$$\varepsilon = 1 - \frac{m}{\pi r^2 h \rho_{tablet}} \quad (2)$$

where r is the tablet radius (mm) and h is the tablet thickness (mm).

Tablet hardness was evaluated using hardness tester (Tablet Tester 8M, Dr. Schleuniger Pharmatron, Switzerland). Tablet hardness can be converted into tensile strength σ_t (MPa), according to Eq. (3).

$$\sigma_t = \frac{2F}{\pi d h} \quad (3)$$

where F is the diametrical crushing force (N), and d is tablet diameter (mm).

2.2.3 Measurement of granule size distribution

The granule size distribution was measured by a sieve analysis method using a vibrating sieve (Vibro, Retsch, Germany), equipped with 1000, 710, 500, 355, 250, 180, 125 and 90 μm sieves.

2.2.4 X-ray microtomography

Synchrotron X-ray microtomography measurements of the tablets were performed at the TOMCAT X02DA beamline of the Swiss Light Source at the Paul Scherrer Institute (Villigen, Switzerland). The X-ray beam produced by the superconducting bending magnet source was monochromatized to a beam energy of 19.9 keV using a large bandwidth (ΔE/E ~ 2%) Ru/C multilayer monochromator. Samples were placed in the essentially parallel X-ray beam about 25 meters from the source. The radiographic projections of the sample were converted to visible light by a 20 μm thick LuAG:Ce scintillator coupled to an optical light microscope with a 10-fold magnification (Optique Peter, France), placed 12 mm downstream of the sample to obtain some degree of edge enhancement for phase contrast reconstructions. The magnified image was recorded using a pco.Edge 5.5 sCMOS camera with 2560 x 2160 pixels (h x v) of 6.5 μm in size, resulting in an effective pixel size of 0.65 μm and a field of view (FOV) of 1.66 mm x 1.40 mm (h x v).

The sample tablets' diameters is significantly larger than the used window for acquisition of projections, therefore only the central parts the tablets were reconstructed with diameter of section equal to 2.0 mm.

Tomographic reconstructions were computed after applying a single distance propagation-based phase contrast filter, using a δ/β ratio of 50, with the gridrec reconstruction algorithm employing a standard ramp filter. This resulted in a sufficiently strong contrast between the components' phases. The volume data was cropped down to 3701 x 3701 pixels in the axial cutting plane during the reconstruction, thus limiting the horizontal extent of the reconstruction to about 2.0 mm.

The preparative processing of the reconstructed data was performed in Image J 1.51j8 (National Institutes of Health, USA) by first binning by factor 4 in all dimensions using an averaging function to reduce the memory footprint necessary for effective computation, followed by a SLIC Superpixels [36] clustering analysis for the segmentation of tablet components. In the resulting multipage TIFF file, the individual components' corresponding pixels were mapped according to their types (e.g., for mefenamic acid the value of 1 was applied) and imported directly into Particle Arrangement and Compaction module of the software.

2.2.5 Disintegration test

The disintegration times were measured using a disintegration tester (Sotax DT3, Sotax AG, Switzerland), according to USP 24 method. Tests were carried out in 900 mL of 50 mM Na-phosphate buffer (pH6.8) containing 1% CTAB at 37°C±0.5 (n=3). All tests were done in triplicate using six tablets for each test.

2.2.6 Dissolution test

Dissolution tests of the tablets were carried out using the USP dissolution apparatus II (AT7smart, Sotax, Switzerland) in 900 mL of 50 mM Na-phosphate buffer (pH6.8) containing 1% CTAB at 37°C±0.5 with a paddle rotation of 75 rpm (n=6). Drug concentrations in the dissolution media were measured by a UV/Vis spectrophotometer (Lambda 25, Perkin Elmer, USA) at wavelength of 294 nm every 5 min.

2.3 Simulation of drug release with cellular automata

2.3.1 Application of Noyes-Whitney equation in numeric calculation of drug dissolution

Drug release calculation model is based on the numeric solution of multiarticulate system defined in three-dimensional space according to the tablet geometry. Tablet geometry is approximated by cubic mesh, the centre of mass for all resulting voxels is in the centre of every cubic mesh element. To calculate the integral drug release from all voxels, the rate of dissolution d_m/d_t from a voxel element representing a solid drug particle surrounded by solvent voxels under sink conditions can be mathematically described according to Eq. (4).

$$d_m/d_t=(A\cdot D)/\lambda\cdot(C_s-C) \quad ,C\rightarrow 0 \text{ (sink condition)} \qquad (4)$$

where voxel contact surface area A (cm2) is $\boldsymbol{A=(1/N)\pi\lambda^2}$, N is the number of neighbours (N=26), diffusion coefficient D (cm²/s) is according to the Stokes-Einstein relation [35], Eq. (5), Cs is the solubility at equilibrium and at experimental temperature, C is the concentration of the solid in the bulk of the dissolution medium at time t. The diffusion coefficient is calculated according to the Eq. (5).

$$D=\frac{1}{f}\cdot\kappa_b\cdot(T+273.15), \qquad (5)$$

where frictional coefficient f for a sphere given by the Stokes' law is $\boldsymbol{f=6\pi\eta R}$ [37], viscosity of water η (Pa·s) is $\eta = 2.414\cdot10^{-5}\cdot10^{247.8/((T+273.15)-140)}$, k_b=1.3806488·10^{-16} (cm^2·kg·s^{-2}·K^{-1}) is Boltzmann constant, T (°C) is temperature, and R (Å) is Stokes radius.

Peer-reviewed version available at Pharmaceutics 2018, 10, 259; doi:10.3390/pharmaceutics10040259

The Stocks-Einstein equation is valid only for limited conditions, and initially was applied for ideal gases. To calculate the realistic diffusion of the molecules in the dissolution medium, the molecular dynamic simulations are used. We employ Desmond 4.8 (D. E. Shaw Research, NY, USA) molecular dynamics simulation for single mefenamic acid molecule in presence of water molecules, at simulated temperature of 310K. The entire root mean deviations (RDMS) of a molecule has been recorded and the diffusion coefficient has been calculated from the slope of the sums of squared displacements (Figure 1, b) according to the Eq. (6) [38]:

$$D = \frac{1}{6}\frac{d}{dt}\sum(|r(t) - r(0)|^2), \quad (6)$$

Where r(t) is the actual molecular displacement in Å^2, and D is coefficient of self-diffusion.

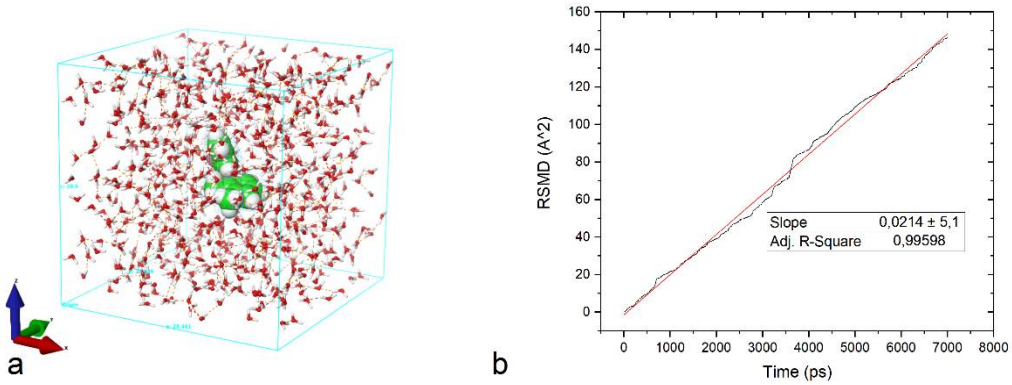

Figure 1. (a) A molecular dynamic setup is shown to simulate the diffusion process of a single molecule of the mefenamic acid in aqueous media. (b) The root squared mean deviations of the target molecule within 7 ns of simulation time. The slope is the first derivative by time and is used to estimate the diffusion coefficient.

The resulting value for the diffusion coefficient of mefenamic acid in water was 3.57e-7 cm^2/s, which is in combination with eq.4 and mass of a single drug voxel yields a C1 value of 22082 (Table 2), i.e., C1 is a voxel mass divided by the rate of the mass transfer from 1/26th of the voxel surface. This constant is used for convenience during simulation, and is just an F-CAD compatible way of describing dissolution kinetics.

The voxel contact surface area is calculated as 1/26 of total voxel area, which is calculated as a surface on an inscribed sphere into the grid element. This assumption is not representing the full complexity of an interface contact between liquid a solid, however allows for sufficiently accurate mass transfer calculation during simulation. The spatial subdivision of the computed voxel into 26 individual interfaces is according to Moor type special neighborhood and is an art of stencil for solving partial differential equations. An increase in number of used voxels, i.e., decrease in the voxel size, improves calculation accuracy yet increases computational costs.

Once the rate of mass migration due to dissolution are calculated with Eq. (4), the mass of every voxel is calculated during the integration step. The integration is carried out by a simple Euler scheme on 26-point stencil, assuming sufficiently small Δt to minimize error.

To reflect the multicomponent nature of a typical pharmaceutical formulation, e.g., different diffusion coefficients and solubilities of its components, the voxels are assigned type information along with physicochemical properties to calculate the mass transfer rates (Eq. 4, 5). The type information is used while traversing the voxel's neighbourhood and calculating mass transfer rate

for every voxel's interface, therefore giving an integral difference value for mass migration at a time t, reflecting the heterogeneous nature of the calculated system.

The above described method, despite its apparent simplicity, is very useful for finding the solutions of a mass distribution function, i.e., a distribution of dissolved and undissolved heterogeneous materials at the defined time intervals. However, this approach is only suitable for simulation of non-disintegrating, non-swelling solid pharmaceutical dosage forms, e.g., lozenges.

To incorporate an effect of tablet disintegration into the simulation algorithm, the concept of state change is applied to each voxel after calculation of the dissolution rates and integration. The algorithm of disintegration modelling consists of X stages:

1. As soon as a disintegrant cell is signalled to get in contact with a medium type voxel, it is state is converted to "active".

2. All "active" disintegrant cells mark their direct neighbours for random scattering within the calculation matrix. The labelling depth, i.e., radius around the active disintegrant particles can be set through the simulations parameter. In this study this parameter was kept to unity.

3. All marked cells are randomly distributed in the surrounding medium to maximize the contact surface to the liquid.

4. As soon as the disintegrant cell is "activated", it loses its action; therefore, the random scattering of its neighbourhood can be fired only once.

The dissolution and disintegration algorithms as described above are realized in using the modelling software package F-CAD v.2.0, Linux Edition (CINCAP GmbH, Switzerland) applying parallel graphical processing units (Kepler architecture) and dedicated libraries (CUDA 9.1) from Nvidia (Palo Alto, CA, USA) to reduce the computation time. The simplicity of the proposed algorithm allows its realization on other computational platforms, such as Python or MATLAB, if the usage of the specialized software is restricted. The size of the voxel matrix was set to 3303 elements, including solid and dissolution medium voxel types. This calculation matrix size was kept for both types of the simulation matrices, the one obtained from microtomography and algorithmically created ones.

For a comparative analysis between the calculated release pattern obtained from microtomography experiments and the algorithmically created calculation matrix the latter was constructed by applying cellular automata algorithms for voxel types. To mimic the granular particle arrangement, i.e., to simulate arrangement of the pre-granulated internal phase within tablet constraints, the "swiss cheese" arrangement procedure was used. In details this method is described in [18], where the initial granular placeholders are enlarged by sequential application of the CA rule [00101110111111111111111111], where a digit position corresponds to the number of neighbour cells containing the type of interest. In other words, this notation can be transformed into a set of 26 production rules, for example:

Rule: If a cell has 3 positive neighbours, then on the next epoch this cell becomes positive.

Rule: If a cell has 2 positive neighbours, then on the next epoch this cell remains unchanged.

The result of the sequential application of the above stated rule for Moor type neighbourhood, on the number of cell triplets randomly distributed in the calculation space results on development of sphere-like objects. These objects, consisting of multiples of individual cells, start to compete for space, therefore, eventually will form a non-uniform size distribution. The rule application is stopped as soon as the size distribution reaches the target values, which were set to correspond to the values

Preprints (www.preprints.org) | NOT PEER-REVIEWED | Posted: 22 October 2018 doi:10.20944/preprints201810.0490.v1

Peer-reviewed version available at Pharmaceutics 2018, 10, 259; doi:10.3390/pharmaceutics10040259

obtained from real granules after high shear granulation. The acceptance range was set to +/- 10% from the average of the real granules.

As soon as the virtual granules were formed, the remaining volumes were blocked by an auxiliary component. The virtual granular material was removed, leaving empty pores in size and shapes of the granules, in other words a negative to granules. The voids were filled with randomly distributed cells corresponding to mefenamic acid, D-mannitol, sodium croscarmellose, hydroxypropyl cellulose, and microcrystalline cellulose. The concentrations of the visual material were kept equal to the values from experimentally obtained granules. As the next step the auxiliary material is removed, and the remaining intergranular voids are filled with the external phase, i.e., remaining amounts of disintegrant and lubricant. In the Figure 2, the resulting matrix is shown in contrast to the microCT of the real tablet.

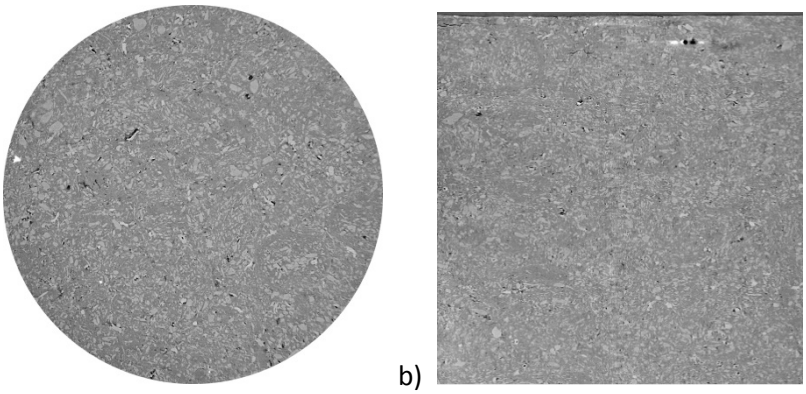

a) b)

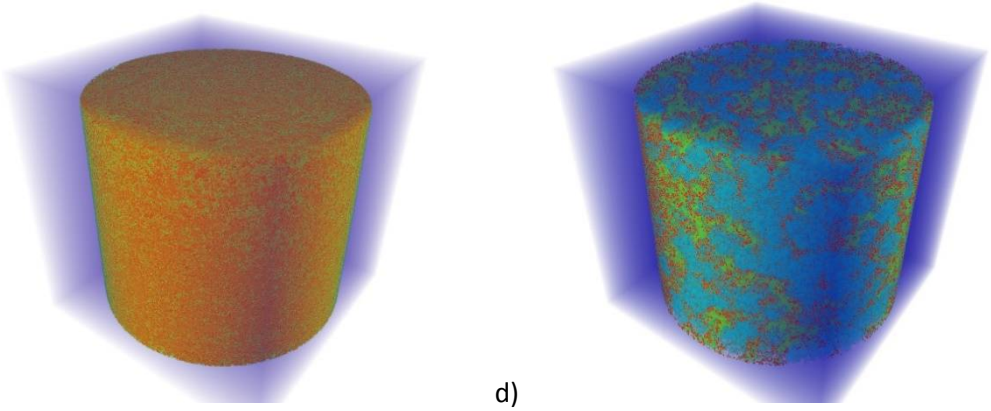

c) d)

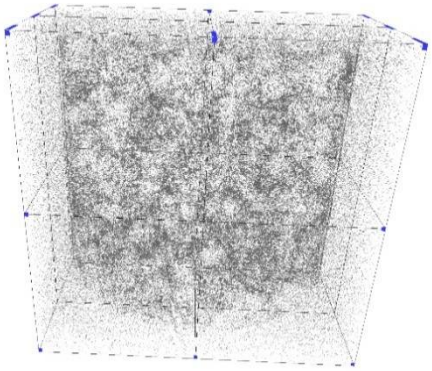

e)

Peer-reviewed version available at Pharmaceutics 2018, 10, 259; doi:10.3390/pharmaceutics10040259

Figure 2. (a) The horizontal cross sectional image of formulation A2 analysed by the microtomography. (b) The vertical cross sectional image of formulation A2 analysed by the microtomography. (c) The results of the volume rendering from microtomographic reconstruction for formulation A2 (red voxel color corresponds to mefenamic acid) and (d) algorithmically created components arrangement (blue voxels correspond to virtual mefenamic acid particles). (e) The skeletonized drawing of the particles distribution (only drug component) is shown after 10 seconds of simulated dissolution.

The values used to calculate the dissolution rate constants for mefenamic acid and other formulation components are summarized in the Table 2.

Table 2. Summary of the parameters used for the *in silico* dissolution simulation

Component	True density (g/cm³)	Type ID	Component code	C_1 constant	C_2 constant
Mefenamic acid	1.2554	1	API	22082	Not applicable
D-mannitol	1.4888	10	Non swelling, soluble filler	200	Not applicable
Microcrystalline cellulose	1.5701	31	Non-swelling or negligible swelling, insoluble fillers	insoluble	Not applicable
Croscarmellose sodium	1.5757	61	Fibrous disintegrant	insoluble	2
Hydroxypropyl cellulose	1.2334	41	Hydrophilic swelling matrix	1e8	1000
Magnesium stearate	1.0539	71	Hydrophobic ingredient	insoluble	Not applicable

2.3.2 Matrices arrangement of tablets

The simulations of the drug release of mefenamic acid tablets were carried out using the software package F-CAD v.2.0. For the simulation of the experimental tablet, the flat-faced round virtual tablets with a diameter of 2 mm were generated. This size was chosen to match the microtomographic acquisition, where the entire tablet scanning was not carried out due to technical limitations. The virtual tablet was discretized into a cubic grid using a voxel side length of 6.5 μm (with 330^3 elements), equal to the microtomographic resolution with voxel side length of 6.5 μm.

2.3.3 Comparison of drug release pattern between experimental and simulated profiles

To evaluate the similarity factor (f_2) between simulated and experimental release profiles, the equation (7) was used [39].

$$f_2 = 50 \cdot \log\left\{\left[1 + \frac{1}{n}\sum_{i=1}^{n}(R_t - T_t)^2\right]^{-0.5} \cdot 100\right\}, \quad (\text{~~1~~}7\text{~~3~~})$$

where n is the number of time points, R_t is the dissolution rate of the experimental tablet at time t, T_t is the dissolution rate of the simulated tablet at time t. A similarity factor (f_2) greater than 50 indicates close correlation between simulated and experimental data.

3. Results

3.1 *In vitro* evaluation of drug release

Peer-reviewed version available at Pharmaceutics 2018, 10, 259; doi:10.3390/pharmaceutics10040259

The properties of the experimental tablets and its compaction condition are summarized in Table 3. *In vitro* drug release of tablets with different porosities were carried out, the results are shown in the Figure 3 for uncompacted granules and tablets.

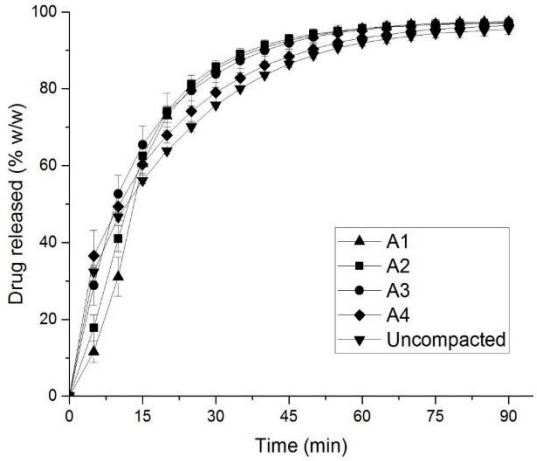

Figure 3. Experimental drug release from mefenamic acid formulations.

As it can be seen from the Figure 3, the release rate is influenced by the tablet porosity, however not for all formulations. The uncompressed granules have very distinctive release profile, quite differentiating from the tablets.

3.2 Granule size distribution experimentally measured and designed in simulation matrixes.

The granule size distribution of the milled granules is shown in Figure 4.

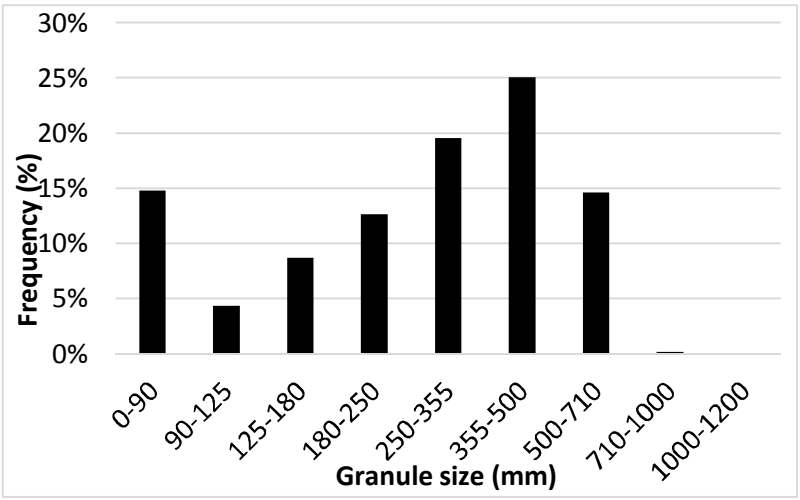

Figure 4. Granule size distribution of mefenamic acid formulation.

The granule size distribution is basically single peak and the sieve fraction of 355-500 μm is greater than any other size fractions, hence the granule size distributions in the algorithmically created matrixes were designed to average 400 μm for formulation A1 to A4.

Peer-reviewed version available at Pharmaceutics 2018, 10, 259; doi:10.3390/pharmaceutics10040259

3.3 Comparison between *in vitro* and *in silico* drug release profiles.

The *in vitro* drug release and *in silico* drug release of the X-ray CT reconstructed tablets and algorithmically created tablets are shown in Fig. 5. The analysis has been carried out for A2 and A3 formulations, due to difficulties to distinguish the material of the tablet components for other studied formulations.

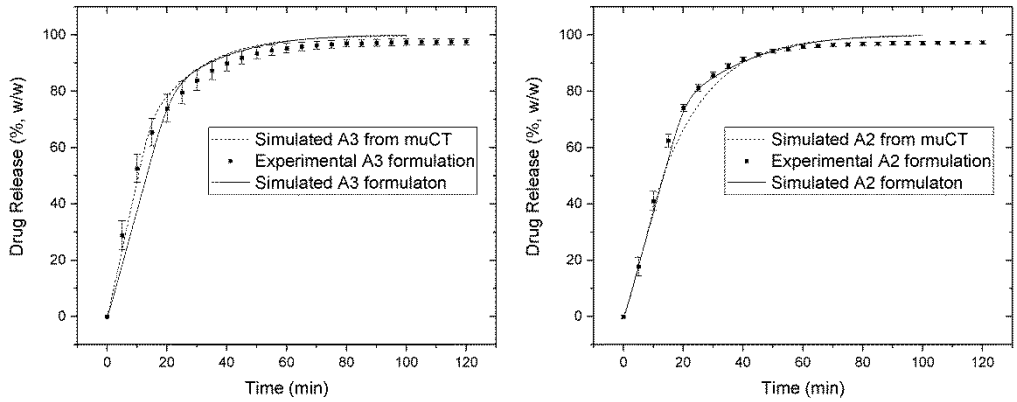

Figure 5. Comparison between *in silico* and *in vitro* release profiles obtained from simulations with algorithmically created tablet component arrangements and the reconstructed matrices with the help of microtomography for formulations A3 (left) and A2 (right).

The obtained similarity factors (f_2) of the dissolution between X-ray reconstructed tablet and experimental tablet are 54 and 72 for formulation A2 and A3, respectively. Also, the obtained similarity factors (f_2) of the dissolution between algorithmically created matrices and experimental tablet are 68 and 73 for A2 and A3, respectively. As demonstrated by the similarity factors (f_2), the dissolution profiles from the X-ray reconstructed tablets and algorithmically created matrices were like those, obtained from the experimental tablets. Important is to keep in mind, that those close correlations are not the results of the fitting but ab initio calculations. These results suggest that the simulation of disintegration and dissolution behaviour with calculation matrix obtained from X-ray microtomography is in good agreement with the experimental tablets.

3.4 *In silico* evaluation of drug release

The *in vitro* and *in silico* drug release of algorithmically created matrices are shown in Figure 6 for formulations A1-A4 and the simulated curves well describe the experimental data. Also, the obtained similarity factors (f_2) are summarized in Table 4 and these are greater than 50, suggesting that the algorithmically created matrices provided the similar drug release to those obtained from the experimental tablets. The simulation dissolution rate calculated with Eq. (4) was set to 1.39e-14 g/s for single contact surface of 9.75e-8 cm^2 under an assumption of unstirred layer thickness equal to 2.6 mm. The necessity to use such large value for an unstirred diffusion layer thickness is dictated by the experimental data [23] and a tendency to produce a cone of powder at the bottom of the dissolution vessel, where mass migration processes are solely diffusion driven. The similarity of the simulated and the experimental results can be seen for calculation with disintegration model, whereas the release profiles simulated without disintegration model resulted in very slow release kinetics (data

Preprints (www.preprints.org) | NOT PEER-REVIEWED | Posted: 22 October 2018 doi:10.20944/preprints201810.0490.v1

Peer-reviewed version available at Pharmaceutics 2018, 10, 259; doi:10.3390/pharmaceutics10040259

not shown). Therefore, this result suggested that the *in silico* simulation with disintegration model produce similar release profile as compared to the *in vitro* evaluation.

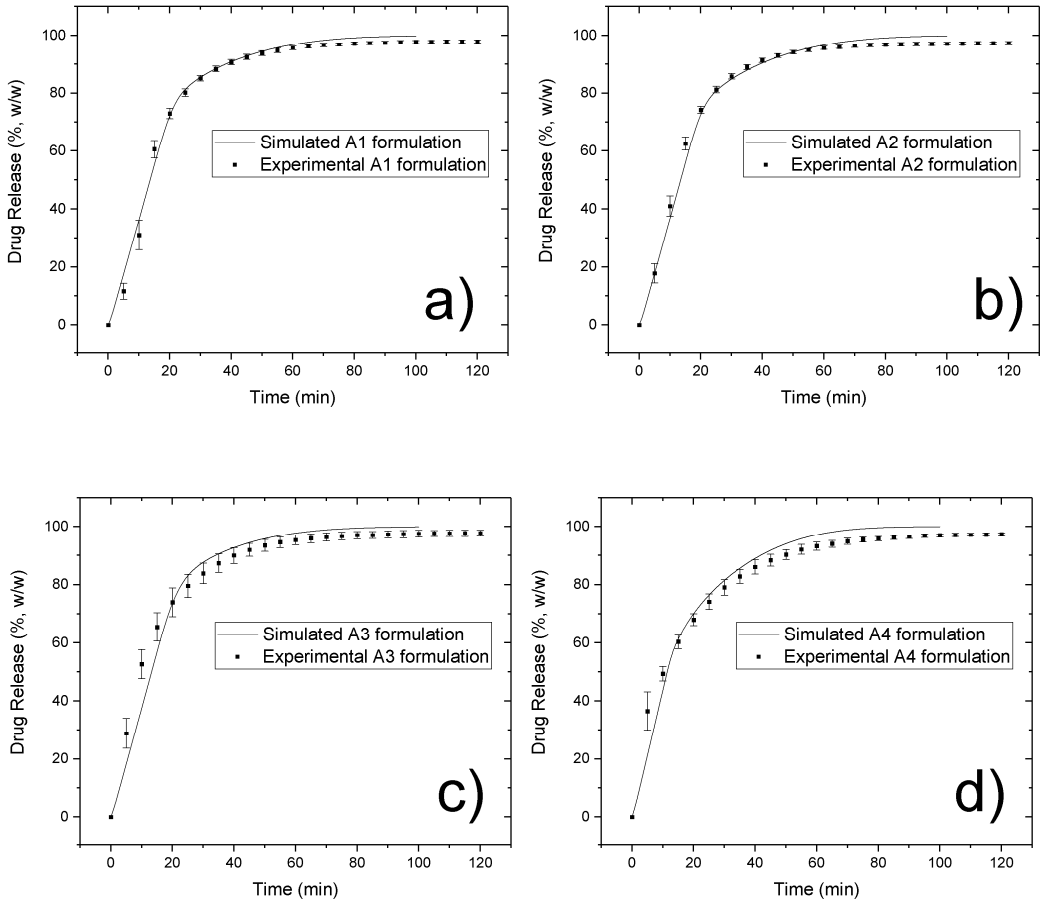

Figure 6. Comparison between simulated release curves obtained from algorithmically created components' arrangements and corresponding experimental data for formulations A1-A4 (a-d).

Table 3. Summary of similarity factors (f_2) between *in vitro* and *in silico* drug release profiles.

Tablet		A1	A2	A3	A4
Similarity factor (f_2)	X-ray reconstructed matrices	NA*	54	72	NA*
	Algorithmically created matrices	67	68	73	71
Porosity (%, v/v)		5.6	9.5	13.7	23.1

*Due to difficulties to distinguish the material of the tablet components, drug release of X-ray reconstructed matrices is not available.

4. Discussion

As *in vitro* results in Figure 3 show, the fast drug release of the formulation at the beginning of the dissolution test is followed by slowed down for all studied formulations. This is an expected behaviour, which correlates with the known theories for disintegration, where tablet porosity serves as medium delivery route to cause the disintegrate particles to start swelling [40,41]. The release rate

Peer-reviewed version available at Pharmaceutics 2018, 10, 259; doi:10.3390/pharmaceutics10040259

from the uncompacted granules is slower than those from the tablets, which is due to depleted action of the intragranular disintegrant, which was mixed with the other components during wet granulation. There are literature data indicating the loss of swelling potential of the disintergrants if they were wet granulated [42]. These findings support the choice of the disintegration model simulation algorithmic steps. Similarly to the existing theories, the "activated" virtual disintegrant cell loses its further potential to force the surrounding components to scatter. In this respect, it is logical to assume that as soon all of the disintegrant in the tablets has swollen, the remaining particles or granules will show different release rate. This effect can be clearly seen on the simulated curves and the experimental results.

As the results in Figure 5 show, the simulated drug release from X-ray reconstructed simulation matrices were like those from the experimental tablets, at the same time the release from the algorithmically created matrices without disintegration simulation show less accurate approximation of the experimental data (data not shown, maximum drug release below 10% was simulated after 60 min). This result suggests that the disintegration and dissolution models are logically close to real physical behaviour and are in good agreement with experiment.

Nowadays it is still quite difficult to access the synchrotron X-ray microCT with sufficient contrast phase information to distinguish between the pharmaceutical formulation components. Therefore, in this study the special attention was payed to compare the release profiles between the matrices created algorithmically with the support from cellular automata and from the tablet microtomography. The results in Figure 5 show that the methods to construct algorithmically the calculation matrix can be used to model the experimental drug release if the disintegration model is engaged. The simulated release profiles amplify the bi-phasic nature of the drug release for low soluble compounds, such as mefenamic acid if the formulation contains partially depleted swelling action disintegrant particles, resulted in the water contact during wet high-shear granulation. As soon as the disintegrant in the external phase is used, the release rate drops to the levels observable from the uncompacted granules. This is well correlated with the existing disintegration theories.

As Figure 6 shows, the engagement of the disintegration algorithm into simulation process results in higher values of similarity factors (f_2) when compared to the simulation without disintegration, including the calculation results from the reconstructed tablets. This suggests that the proposed *in silico* disintegration procedure is in a good agreement with the experiment. However, still the existing deviation between the *in vitro* and *in silico* drug release suggest that there are more subtle mechanisms contributes to the studied processes, for example, change in granule particle size during compaction, percolation effects or wicking between the disintegrant fibres. When comparing the *in vitro* drug release of formulation A3, A4 and uncompacted granules as shown in Figure 3, the formulations compacted at higher compressive stresses (i.e. 99 MPa, formulation A3), showed a faster drug release than formulation A4 compacted at lower compressive stress (i.e. 45 MPa). Similar behaviour is reported for the uncompressed granules. For this reason, it can be thought that the granules were damaged during the compaction process and the produced fine fractions resulted in faster drug release profiles. Compressive stress seems to play an important role in maintaining granulometric composition within a tablet, which is well supported in the literature [43–45]. However, the damage to granular structures after compressive stress application cannot be seen on the microtomographic acquisitions from these tablets. On contrary, the unchanged granular patterns can be seen in the consecutive cross sectional images (a part of the horizontal and vertical cross sectional images shown in Figure 2). Therefore, further investigations to consider the influence of the compression dwell time, the material mechanical properties and the behaviour of granular breakage may be necessary for a better understanding the effect of granular partitioning on the disintegration and release rates.

The algorithm for modelling and simulation of the disintegration behaviour proposed and evaluated in this study can be considered as tool to elucidate the influences of material attributes of

tablets and process parameters on drug release and can become a useful aid in process and formulation development, especially for bioavailability enhancement of the low soluble compounds, quality assurance, and generally in drug product development.

5. Conclusions

The disintegration model proposed in this study is a first approximation attempt to construct the comprehensive simulation tool to be used in the pharmaceutical development. The proposed model is not featuring the fine mechanics of all acting forces superpositions during the wetting, onset on swelling and final dissertation of the tablet. The used distribution approach of the disintegrated particles is far from reality, however even these crude approximations are improving the simulation model performance.

Future work on accommodating the mechanical forces actions with either soft particles hydrodynamics or rigid colliding spheres may bring more insides on the understating the fine mechanics of the process of tablet disintegration.

Author Contributions: For research articles with several authors, a short paragraph specifying their individual contributions must be provided. The following statements should be used "conceptualization, R. Yokoyama and G. Kimura; methodology, R. Yokoyama and C. Schlepütz; study concept and simulation software, M. Puchkov; data curation, R. Yokoyama and M. Puchkov; writing—original draft preparation, R.Yokoyama; writing—review and editing, M. Puchkov.

Acknowledgments: The authors thank Shionogi & Co., LTD. for financial support and Mr. Darryl Borland for editorial assistance.

Conflicts of Interest: The authors declare no conflict of interest.

References

1. Siepmann, J.; Siepmann, F. Mathematical modeling of drug dissolution. *Int. J. Pharm.* **2013**, *453*, 12–24, doi:10.1016/j.ijpharm.2013.04.044.
2. Macheras, P.; Iliadis, A. *Modeling in Biopharmaceutics, Pharmacokinetics, and Pharmacodynamics*; Interdisciplinary Applied Mathematics; Springer-Verlag: New York, 2006; Vol. 30; ISBN 0-387-28178-9.
3. Wu, C.-Y.; Ruddy, O. M.; Bentham, A. C.; Hancock, B. C.; Best, S. M.; Elliott, J. A. Modelling the mechanical behaviour of pharmaceutical powders during compaction. *Powder Technol.* **2005**, *152*, 107–117, doi:10.1016/j.powtec.2005.01.010.
4. Lamberti, G.; Galdi, I.; Barba, A. A. Controlled release from hydrogel-based solid matrices. A model accounting for water up-take, swelling and erosion. *Int. J. Pharm.* **2011**, *407*, 78–86, doi:10.1016/j.ijpharm.2011.01.023.
5. Kimber, J. A.; Kazarian, S. G.; Štěpánek, F. DEM simulation of drug release from structurally heterogeneous swelling tablets. *Powder Technol.* **2013**, *248*, 68–76, doi:10.1016/j.powtec.2012.12.039.
6. Kimber, J. A.; Kazarian, S. G.; Štěpánek, F. Modelling of pharmaceutical tablet swelling and dissolution using discrete element method. *Chem. Eng. Sci.* **2012**, doi:10.1016/j.ces.2011.10.066.

7. Kimber, J. A.; Kazarian, S. G.; Štěpánek, F. Formulation design space analysis for drug release from swelling polymer tablets. *Powder Technol.* **2013**, *236*, 179–187, doi:10.1016/j.powtec.2012.02.027.
8. Kimber, J. A.; Kazarian, S. G.; Štěpánek, F. Microstructure-based mathematical modelling and spectroscopic imaging of tablet dissolution. *Comput. Chem. Eng.* **2011**, *35*, 1328–1339, doi:10.1016/j.compchemeng.2010.07.008.
9. Thornton, C.; Ciomocos, M. T.; Adams, M. J. Numerical simulations of agglomerate impact breakage. *Powder Technol.* **1999**, *105*, 74–82, doi:10.1016/S0032-5910(99)00120-5.
10. Mishra, B. K.; Thornton, C. Impact breakage of particle agglomerates. *Int. J. Miner. Process.* **2001**, *61*, 225–239, doi:10.1016/S0301-7516(00)00065-X.
11. Bagherzadeh-Khalkhali, A.; Mirghasemi, A. A.; Mohammadi, S. Micromechanics of breakage in sharp-edge particles using combined DEM and FEM. *Particuology* **2008**, *6*, 347–361, doi:10.1016/j.partic.2008.07.002.
12. Frenning, G. An efficient finite/discrete element procedure for simulating compression of 3D particle assemblies. *Comput. Methods Appl. Mech. Eng.* **2008**, *197*, 4266–4272, doi:10.1016/j.cma.2008.05.002.
13. Kimber, J. A.; Kazarian, S. G.; Štěpánek, F. Modelling of pharmaceutical tablet swelling and dissolution using discrete element method. *Chem. Eng. Sci.* **2012**, *69*, 394–403, doi:10.1016/j.ces.2011.10.066.
14. Ketterhagen, W. R.; AM Ende, M. T.; Hancock, B. C. Process modeling in the pharmaceutical industry using the discrete element method. *J. Pharm. Sci.* **2009**, *98*, 442–470, doi:10.1002/jps.21466.
15. Kodam, M.; Curtis, J.; Hancock, B.; Wassgren, C. Discrete element method modeling of bi-convex pharmaceutical tablets: Contact detection algorithms and validation. *Chem. Eng. Sci.* **2012**, *69*, 587–601, doi:10.1016/j.ces.2011.11.011.
16. Rybacki, S.; Himmelspach, J.; Uhrmacher, A. M. Experiments with Single Core, Multi-core, and GPU Based Computation of Cellular Automata. *2009 First Int. Conf. Adv. Syst. Simul.* **2009**, 62–67, doi:10.1109/SIMUL.2009.36.
17. Stephen Wolfram: A New Kind of Science.
18. Puchkov, M.; Tschirky, D.; Leuenberger, H. 3-D cellular automata in computer-aided design of pharmaceutical formulations: Mathematical concept and F-CAD software. In *Formulation Tools for Pharmaceutical Development*; 2013; pp. 155–201 ISBN 9781907568992.
19. Laaksonen, H.; Hirvonen, J.; Laaksonen, T. Cellular automata model for swelling-controlled drug release. *Int. J. Pharm.* **2009**, *380*, 25–32, doi:10.1016/j.ijpharm.2009.06.023.
20. Kimura, G.; Puchkov, M.; Leuenberger, H. An attempt to calculate *in silico* disintegration time of tablets containing mefenamic acid, a low water-soluble drug. *J. Pharm. Sci.* **2013**, *102*, 2166–78, doi:10.1002/jps.23541.
21. Eberle, V. A.; Schoelkopf, J.; Gane, P. A. C.; Alles, R.; Huwyler, J.; Puchkov, M. Floating gastroretentive drug delivery systems:Comparison of experimental and simulated dissolution profiles and floatation behavior. *Eur. J. Pharm. Sci.* **2014**, *58*, 34–43, doi:10.1016/j.ejps.2014.03.001.

22. Eberle, V. A.; Häring, A.; Schoelkopf, J.; Gane, P. A. C.; Huwyler, J.; Puchkov, M. *In silico* and *in vitro* methods to optimize the performance of experimental gastroretentive floating mini-tablets *In silico* and *in vitro* methods to optimize the performance of experimental gastroretentive floating mini-tablets. **2015**, *9045*, doi:10.3109/03639045.2015.1078350.
23. Park, S.-H.; Choi, H.-K. The effects of surfactants on the dissolution profiles of poorly water-soluble acidic drugs. *Int. J. Pharm.* **2006**, *321*, 35–41, doi:10.1016/j.ijpharm.2006.05.004.
24. Razvi, N.; Siddiqui, S. A.; Khan, L. G. The effect of surfactant on the dissolution rate of ibuprofen tablets. *IntI. Chern. Pharm. Med. J* **2005**, *2*, 213–216.
25. Kitamori, N.; Makino, T. Effect of drug content and drug particle size on the change in particle size during tablet compression. *J. Pharm. Pharmacol.* **1979**, *31*, 505–507, doi:10.1111/j.2042-7158.1979.tb13572.x.
26. Yekpe, K.; Abatzoglou, N.; Bataille, B.; Gosselin, R.; Sharkawi, T.; Simard, J.-S.; Cournoyer, A. Predicting the dissolution behavior of pharmaceutical tablets with NIR chemical imaging. *Int. J. Pharm.* **2015**, *486*, 242–251, doi:10.1016/j.ijpharm.2015.03.060.
27. Ghayas, S.; Sheraz, M. A.; Anjum, F.; Baig, M. T. Factors influencing the dissolution testing of drugs. *Pak. J. Heal. Res.* **2013**, *1*, 1–11.
28. Yen, J. K. The dissolution rate principle in practical tablet formulation. *Can. Pharm. J.* **1964**, *97*, 493–499.
29. Desai, P. M.; Liew, C. V.; Heng, P. W. S. Review of Disintegrants and the Disintegration Phenomena. *J. Pharm. Sci.* 2016.
30. Steendam, R.; Frijlink, H. W.; Lerk, C. F. Plasticisation of amylodextrin by moisture. Consequences for compaction behaviour and tablet properties. *Eur. J. Pharm. Sci.* **2001**, *14*, 245–54.
31. Sinka, I. C.; Burch, S. F.; Tweed, J. H.; Cunningham, J. C. Measurement of density variations in tablets using X-ray computed tomography. *Int. J. Pharm.* **2004**, *271*, 215–224, doi:10.1016/j.ijpharm.2003.11.022.
32. Busignies, V.; Leclerc, B.; Porion, P.; Evesque, P.; Couarraze, G.; Tchoreloff, P. Quantitative measurements of localized density variations in cylindrical tablets using X-ray microtomography. *Eur. J. Pharm. Biopharm.* **2006**, *64*, 38–50, doi:10.1016/j.ejpb.2006.02.007.
33. Pajander, J.; Vanveen, B.; Korhonen, O.; Lappalainen, R.; Ketolainen, J. Liquid boundary movements in cylindrical and convex hydrophobic matrix tablets: Effects on tablet cracking and drug release. *Eur. J. Pharm. Biopharm.* **2006**, *64*, 167–172, doi:10.1016/j.ejpb.2006.05.011.
34. Westermarck, S.; Juppo, A. M.; Kervinen, L.; Yliruusi, J. Pore structure and surface area of mannitol powder, granules and tablets determined with mercury porosimetry and nitrogen adsorption. *Eur. J. Pharm. Biopharm.* **1998**, *46*, 61–68, doi:10.1016/S0939-6411(97)00169-0.
35. Smrčka, D.; Dohnal, J.; Štěpánek, F. Dissolution and disintegration kinetics of high-active pharmaceutical granules produced at laboratory and manufacturing scale. *Eur. J. Pharm. Biopharm.* **2016**, doi:10.1016/j.ejpb.2016.04.005.
36. Shah-hosseini, H. SLIC Superpixels Compared to State-of-the-Art Superpixel Methods. *IEEE Trans. Pattern Anal. Mach. Intell.* **2002**, *24*, 1388–1393, doi:10.1109/TPAMI.2012.125.
37. Hansen, S. Translational friction coefficients for cylinders of arbitrary axial ratios estimated by Monte Carlo simulation. *J. Chem. Phys.* **2004**, *121*, 9111–9115, doi:10.1063/1.1803533.

38. Amirjalayer, S.; Tafipolsky, M.; Schmid, R. Molecular Dynamics Simulation of Benzene Diffusion in MOF-5: Importance of Lattice Dynamics. *Angew. Chemie Int. Ed.* **2007**, *46*, 463–466, doi:10.1002/anie.200601746.
39. Food and Drug Administration (FDA) Centre for Drug Evaluation and Research (CDER) Guidance for Industry Guidance for Industry Dissolution Testing of Immediate. **1997**, *4*, 15–22.
40. Yassin, S.; Goodwin, D. J.; Anderson, A.; Sibik, J.; Wilson, D. I.; Gladden, L. F.; Zeitler, J. A. The Disintegration Process in Microcrystalline Cellulose Based Tablets, Part 1: Influence of Temperature, Porosity and Superdisintegrants. *J. Pharm. Sci.* **2015**, *104*, 3440–3450, doi:10.1002/jps.24544.
41. Bi, Y. X.; Sunada, H.; Yonezawa, Y.; Danjo, K. Evaluation of rapidly disintegrating tablets prepared by a direct compression method. *Drug Dev. Ind. Pharm.* **1999**, doi:10.1081/DDC-100102211.
42. Gould, P. L.; Tan, S. Bin The effect of recompression on the dissolution of wet massed tablets containing "super" disintegrants. *Drug Dev. Ind. Pharm.* **1986**, doi:10.3109/03639048609042618.
43. García-Armenta, E.; Téllez-Medina, D. I.; Alamilla-Beltrán, L.; Arana-Errasquín, R.; Hernández-Sánchez, H.; Gutiérrez-López, G. F. Multifractal breakage patterns of thick maltodextrin agglomerates. *Powder Technol.* **2014**, *266*, 440–446, doi:10.1016/j.powtec.2014.06.047.
44. Yap, S. F.; Adams, M. J.; Seville, J. P. K.; Zhang, Z. Single and bulk compression of pharmaceutical excipients: Evaluation of mechanical properties. *Powder Technol.* **2008**, *185*, 1–10, doi:10.1016/j.powtec.2007.09.005.
45. Duberg, M.; Nyström, C. Studies on direct compression of tablets XVII. Porosity—pressure curves for the characterization of volume reduction mechanisms in powder compression. *Powder Technol.* **1986**, *46*, 67–75, doi:10.1016/0032-5910(86)80100-0.